

Antireflection gratings for a photonic-crystal flat lens

Wojciech Śmigaj, Boris Gralak,* Raphaël Pierre, and Gérard Tayeb

Institut Fresnel, CNRS, Aix-Marseille Université, Ecole Centrale Marseille, Campus de St Jérôme,
13397 Marseille Cedex 20, France

*Corresponding author: boris.gralak@fresnel.fr

Received September 3, 2009; revised October 12, 2009; accepted October 12, 2009;
posted October 15, 2009 (Doc. ID 116611); published November 11, 2009

A dielectric structure with effective permittivity and permeability close to -1 operating for propagative waves at optical wavelengths is proposed. This structure is a two-dimensional photonic crystal with refractive index -1 , coated by appropriate antireflection gratings. Numerical simulations involving a flat lens made of this optimized crystal illustrate the improvements that antireflection gratings can bring. In particular, following Veselago's proposition, this lens "can focus at a point the radiation from a point source" with negligible reflection losses. The proposed design takes into account the fabrication requirements and can be used for optical devices integrated in planar waveguides. © 2009 Optical Society of America
OCIS codes: 050.5298, 260.2110, 220.3630.

Negative-index media (NIM) [1] may become vital ingredients of next-generation optical devices with novel capabilities [2–4]. Homogeneous materials with such properties—simultaneously negative permittivity and permeability—do not exist in nature, but metamaterials like periodic metallic structures can mimic them when appropriate conditions are fulfilled [5–7]. In addition, theoretical [8,9] and experimental [6,10,11] results have confirmed that purely dielectric photonic crystals (PCs) can behave like negative refractive-index materials.

In the optical domain, subwavelength resolution and perfect lens concepts [2] become difficult to achieve because of absorption in metallic structures [12] and the limited range of permittivities available in PCs [13]. However, the latter are certainly good candidates for the original flat lens proposed by Veselago [1,4], which is based solely on the propagative waves, and "can focus at a point the radiation from a point source" without reflection losses. Thus all that follows concerns this ordinary focusing ability, in which evanescent waves play no part.

Negative refraction in PCs is now a well-known phenomenon, obtained when the shape of their dispersion law is appropriate [9,14]. Nevertheless, negative-refractive-index PCs embedded in air suffer from reflection losses at surfaces. In terms of effective negative permittivity ϵ and permeability μ , this can be interpreted by refractive index $(\epsilon\mu)^{1/2}$ equal to -1 but impedance $(\mu/\epsilon)^{1/2}$ different from the one of air [15,16]. Moreover, it has been observed that the PC's reflectivity can be influenced by restructuring the crystal's surface [13,17–19]. In our opinion, however, the antireflection solutions proposed to date are not fully satisfactory.

Some of them [20] apply mainly to PCs made of dielectric rods in air (and thus cannot be used in integrated versions of optical devices) or rely on the presence of very thin slits, undoubtedly difficult to fabricate [21]. In turn, antireflection coatings, advocated in [22], are simple and elegant but unfortunately have restricted angular tolerance. Yet another

solution [17,23] is to scan the possible natural cuts of the infinite PC in search of the one giving the smallest reflections. This usually yields easily fabricable structures, but the achievable performance is limited by the fact that there is only a single degree of freedom available. In this letter, we intend to fill this gap by proposing realistic and efficient wide-angle antireflection gratings (AGs) to be etched on the input and output surfaces of PC lenses.

Our aim is to design a structure with properties imagined by Veselago and applicable in optical devices integrated in planar waveguides [11,23]. The starting point—what we shall call the *original crystal*—is a two-dimensional PC made of a hexagonal lattice of circular air holes with radius r , drilled in a matrix with permittivity $\epsilon_m = 10.6$. This value of ϵ_m corresponds to the effective index of the fundamental guided mode of planar waveguides comprising the semiconductors InP and GaInAsP used in earlier experimental works [11]. We consider s polarization, i.e., the electric field is parallel to the axis of holes. For $r = 0.365a$, where a denotes the lattice constant, the dispersion curves of such a crystal imply an NIM behavior within the second band; the effective refractive index of the PC approaches -1 near the frequency $\omega_0 = 0.311 \times 2\pi c/a$.

We turn now to the system composed of the original crystal and some AG superimposed on its surface. Here we focus on trapezoidal AGs since they can be easily etched by electron-beam lithography. The trapezoidal "tooth" is defined by four parameters (Fig. 1): w_b , w_t , h_b , and h_t . The grating period is set to the PC lattice constant a and the trapezoid permittivity to ϵ_m .

The values of the geometrical parameters w_b , w_t , h_b , and h_t are determined by an optimization procedure described in detail in [24] and briefly recalled below. First, it is important to choose the original crystal's termination plane in such a way that the effective-medium description of the PC is as accurate as possible. On the basis of the results obtained in

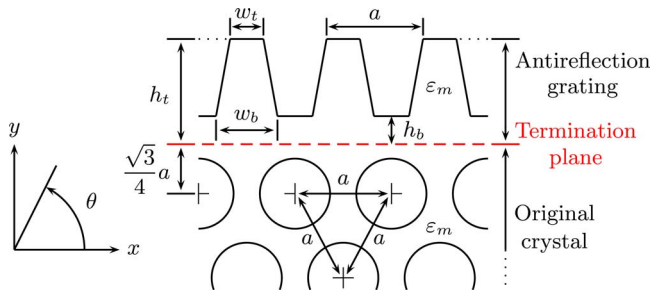


Fig. 1. (Color online) Photonic crystal with its surface covered by an antireflection grating.

our earlier work [15,16,18], we conclude that this is the case for the plane lying midway between two horizontal rows of holes, as shown in Fig. 1 (dashed line). Assuming now that the semi-infinite PC can be considered as an effective homogeneous medium [18], we can make its reflectivity vanish for a given incidence by adding a homogeneous coating layer. This layer is then replaced by a lamellar grating (i.e., $w_b = w_t$ and $h_b = 0$) with geometry (w_b and h_t) found analytically using the effective-medium theory described in [25]. Finally, this grating is used as the starting point in an optimization procedure that minimizes the averaged reflectivity in a wide range of incidences. In the present case, it leads to the trapezoidal profile defined by $w_t = 0.22a$, $w_b = 0.29a$, $h_t = 0.53a$, and $h_b = 0.08a$. In the following, the original crystal covered with this grating will be called the *optimized crystal*.

Figure 2 shows the angular dependence of the reflectivity R of the original and optimized crystals. The former is highly reflective: $R > 0.25$ throughout the range of propagative incident waves. In contrast, the reflectivity of the optimized PC does not exceed 0.05 over a wide range of incidence angles (up to about 60°) and is still relatively low for higher angles. This clearly indicates an AG's capability to suppress undesirable reflected light.

We shall now investigate the influence of the proposed AG on the performance of a (finite) PC flat lens (see Fig. 3). As demonstrated in Fig. 2, the upper AG enhances transmission from air to the crystal and, by reciprocity, the lower one enhances transmission from the crystal to air. We take $a = 482$ nm to make our working frequency ω_0 correspond to the telecommunications wavelength $\lambda_0 = 1.55$ μm .

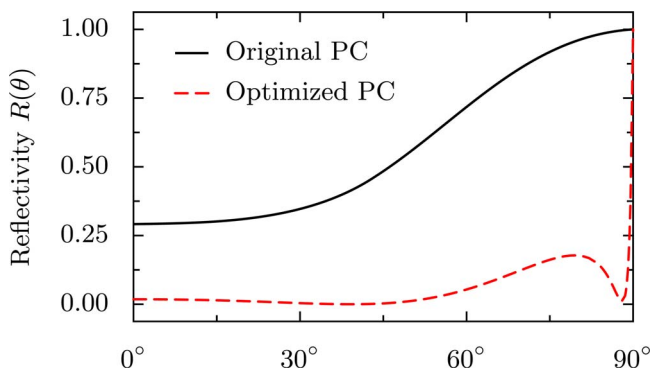


Fig. 2. (Color online) Reflectivities as functions of the angle of incidence.

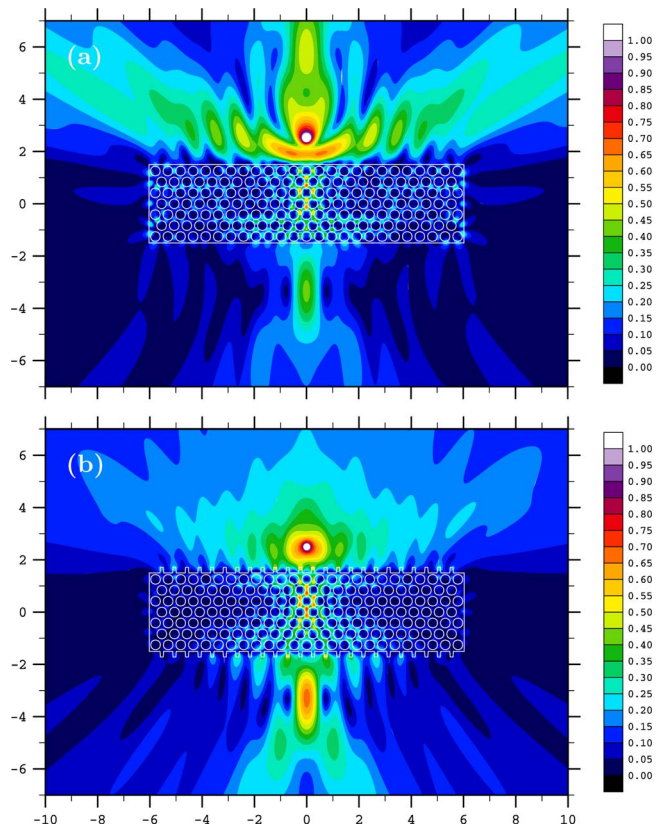


Fig. 3. (Color online) Modulus of the electric field around (a) the original flat lens and (b) the optimized flat lens with trapezoidal AGs. The flat lenses are embedded in air. Spatial coordinates are in micrometers. Wavelength, $\lambda_0 = 1.55$ μm .

For numerical calculations, we use a code based on the fictitious sources method combined with the scattering matrix method [26]. Figure 3 shows the modulus of the electric field generated by a wire source located at $(x, y) = (0, 2.5$ $\mu\text{m})$. As expected, owing to negative refraction, images of the wire source appear inside and below the flat lens.

With AGs present, the field within the image zone reaches 0.68 [Fig. 3(b)], while without AGs it does not exceed 0.42 [Fig. 3(a)]. In addition, from Fig. 3(b), the radiation is almost isotropic into the half-plane above the lens; this corroborates the good antireflection performance of the proposed grating.

Another way to witness the efficiency of the optimized system consists in comparing the far-field intensity $I(\theta)$ of the field scattered by the two lenses. For the angle θ defined in Fig. 1 taken in $[0^\circ, 180^\circ]$, $I(\theta)$ gives the repartition of the power scattered into the upper half plane. To perform the comparison, the two far-field intensities are averaged over the interval $[30^\circ, 150^\circ]$ (grazing angles are ignored, since they are irrelevant owing to the finite width of the lens). As expected, the averaged $I(\theta)$ of the original lens, 0.559, is much larger than that of the optimized lens, 0.019.

As an illustration of the gain brought by AGs, we present a nonsimplistic example involving the optimized flat lens. We attach a cylinder with diameter 1.5 μm and permittivity ϵ_m at the bottom of the lens (Fig. 4).

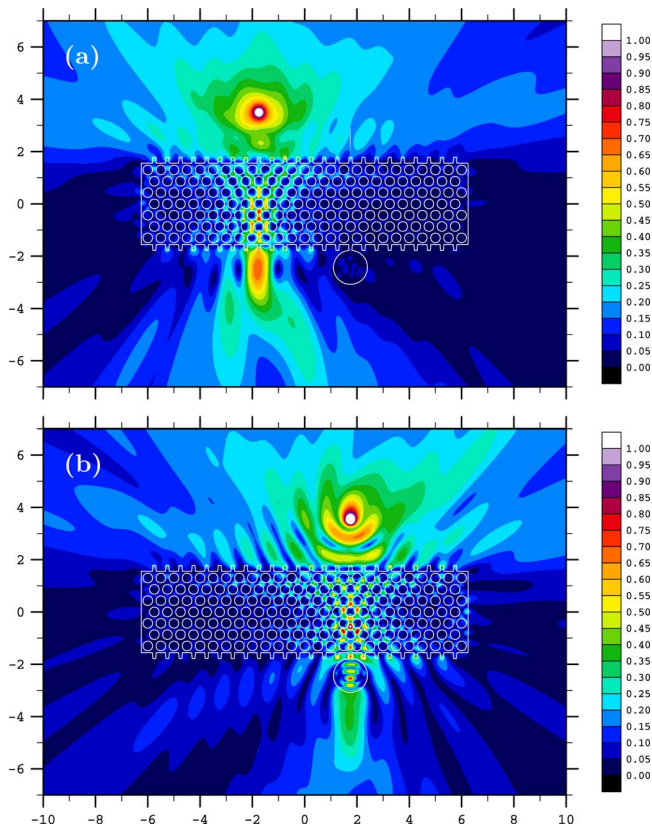


Fig. 4. (Color online) Optimized flat lens with an attached object: (a) object in the blind zone, (b) object at focus.

First, we consider the situation where the wire source is located at $(-1.75, 3.5) \mu\text{m}$. In this case, the image formed by the lens is far away from the object [Fig. 4(a)] and thus does not interact strongly with it. As shown in Fig. 4(b), however, the field distribution above the lens changes drastically when the wire source is shifted to $(1.75, 3.5) \mu\text{m}$, directly above the object.

The change is even more apparent on the $I(\theta)$ plot (Fig. 5), providing a quantitative criterion. When the object is in the blind zone, $I(\theta)$ stays below 0.1 over the interval $[30^\circ, 150^\circ]$, with the average value equal to 0.026. On the other hand, when the image impinges on the object, the averaged $I(\theta)$ is ten times greater: 0.258.

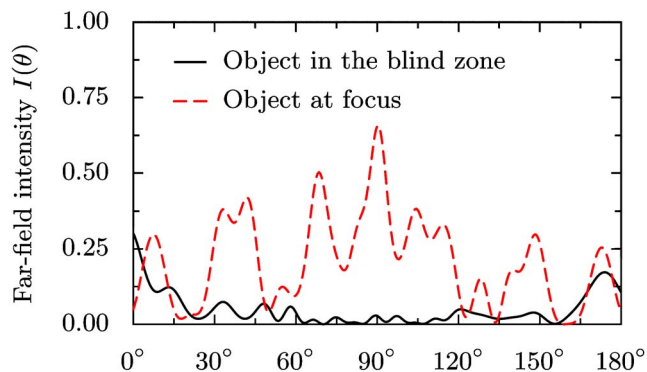


Fig. 5. (Color online) Far-field intensity for situations of Fig. 4.

To conclude, we have proposed an antireflection grating permitting to reduce significantly the reflectivity of a photonic crystal. The resulting structure is, for almost all propagative waves, a good approximation of the perfect medium with index -1 , i.e., a medium with effective refractive index close to -1 and impedance close to the vacuum one [15,16]. We have also demonstrated the application of the optimized flat lens made of the proposed photonic crystal for the purposes of imaging and object detection. Our solution takes into account the fabrication requirements of electron beam lithography.

This work was partly supported by the project FANI (grant ANR-07-NANO-038-03) funded by the Agence Nationale de la Recherche.

References

1. V. G. Veselago, *Sov. Phys. Usp.* **10**, 509 (1968).
2. J. B. Pendry, *Phys. Rev. Lett.* **85**, 3966 (2000).
3. S. Guenneau, B. Gralak, and J. B. Pendry, *Opt. Lett.* **30**, 1204 (2005).
4. V. Veselago, L. Braginsky, V. Shklover, and C. Hafner, *J. Comput. Theor. Nanosci.* **3**, 1 (2006).
5. D. R. Smith, W. J. Padilla, D. C. Vier, S. C. Nemat-Nasser, and S. Schultz, *Phys. Rev. Lett.* **84**, 4184 (2000).
6. K. Aydin, I. Bulu, and E. Ozbay, *Appl. Phys. Lett.* **90**, 254102 (2007).
7. N. Liu, H. Guo, L. Fu, S. Kaiser, H. Schweizer, and H. Giessen, *Nature Mater.* **7**, 31 (2008).
8. M. Notomi, *Phys. Rev. B* **62**, 10696 (2000).
9. B. Gralak, S. Enoch, and G. Tayeb, *J. Opt. Soc. Am. A* **17**, 1012 (2000).
10. E. Cubukcu, K. Aydin, E. Ozbay, S. Foteinopoulou, and C. M. Soukoulis, *Nature* **423**, 604 (2003).
11. N. Fabre, L. Lalouat, B. Cluzel, X. Mélique, D. Lippens, F. de Fornel, and O. Vanbésien, *Phys. Rev. Lett.* **101**, 073901 (2008).
12. N. Garcia and M. Nieto-Vesperinas, *Phys. Rev. Lett.* **88**, 207403 (2002).
13. C. Luo, S. G. Johnson, J. D. Joannopoulos, and J. B. Pendry, *Phys. Rev. B* **68**, 045115 (2003).
14. S. Foteinopoulou and C. M. Soukoulis, *Phys. Rev. B* **67**, 235107 (2003).
15. T. Decoopman, G. Tayeb, S. Enoch, D. Maystre, and B. Gralak, *Phys. Rev. Lett.* **97**, 073905 (2006).
16. R. Pierre and B. Gralak, *J. Mod. Opt.* **55**, 1759 (2008).
17. S. Xiao, M. Qiu, Z. Ruan, and S. He, *Appl. Phys. Lett.* **85**, 4269 (2004).
18. W. Śmigaj and B. Gralak, *Phys. Rev. B* **77**, 235445 (2008).
19. Z. Lu and D. Prather, *Opt. Express* **15**, 8340 (2007).
20. Y. Jin and S. He, *Phys. Lett. A* **90**, 174113 (2007).
21. B. Zhang and M. Li, *Eur. Phys. J. D* **45**, 321 (2007).
22. Z. Li, E. Ozbay, H. Chen, J. Chen, F. Yang, and H. Zheng, *J. Phys. D* **40**, 5873 (2007).
23. B. D. F. Casse, W. T. Lu, R. K. Banyal, Y. J. Huang, S. Selvarasah, M. R. Dokmeci, C. H. Perry, and S. Sridhar, *Opt. Lett.* **34**, 1994 (2009).
24. W. Śmigaj, R. Pierre, B. Gralak, and G. Tayeb, in *SPP4 Surface Plasmon Photonics Conference* (2009).
25. D. Raguin and G. Morris, *Appl. Opt.* **32**, 2582 (1993).
26. G. Tayeb and S. Enoch, *J. Opt. Soc. Am. A* **21**, 1417 (2004).